

Crystal Structures of Nylon 5,6. A Model with Two Hydrogen Bond Directions for Nylons Derived from Odd Diamines

J. Puiggali,* L. Franco, C. Alemán, and J. A. Subirana

Departament d'Enginyeria Química, ETS d'Enginyers Industrials, Universitat Politècnica de Catalunya, Diagonal 647, Barcelona 08028, Spain

Received December 30, 1997; Revised Manuscript Received May 7, 1998

ABSTRACT: Two crystalline structures for nylon 5,6 have been studied by transmission electron microscopy, electron diffraction, and X-ray diffraction. A γ form or an α -like phase can be obtained as a function of the method used to prepare the sample. Structural modeling and energy calculations have been carried out for the second form. Results point to a structure with two hydrogen bond directions as recently postulated for even–odd nylons and odd polyoxamides. It appears therefore that in even–odd and odd–even nylons an α -like structure may be frequently observed, but with two hydrogen bond directions. Our results strongly favor for nylon 5,6 a model in which the methylenes are in an all-trans conformation, while the torsional angles for the $\text{CH}_2\text{--NH}$ and $\text{CH}_2\text{--CO}$ bonds of one residue respectively are $\varphi = +152^\circ$ and $\psi = \pm 137^\circ$. Temperature-induced structural changes have also been studied for nylon 5,6 fibers. Pseudohexagonal packing is obtained near 220°C in a process which takes place without changes in the hydrogen bond system.

Introduction

Nylons have two main types of stable crystal structures, which are named α and γ forms. Although additional polymorphs exist, they can be classified as variations of these main structures. The α form is characteristic of both even nylons with a low number of methylene groups and even–even nylons. This structure, described by Bunn and Garner¹ for the first time (nylon 6,6), is characterized by a fully extended planar zigzag conformation of the molecular chains. These chains form parallel planar sheets of hydrogen bonded molecules. Diffraction patterns are characterized by two intense reflections at ca. 4.4 and 3.7 Å, which are related to the spacings between the crystallographic planes constituted by non-hydrogen-bonded and hydrogen-bonded molecules, respectively.

The γ form was initially suggested by Kinoshita² (nylon 7,7) as a explanation of the experimental evidence for complete hydrogen bond formation in nylons m,n derived from odd diamines and/or odd diacids. In addition, nylons n (with n odd and also even ≥ 6) give the same kind of structure. In these cases the molecular configuration is characterized by torsion angles near $\pm 120^\circ$ for the bonds adjacent to the amide groups. As a consequence, (i) the chain repeat distance is shortened about 0.35 Å/amide group with respect to the extended conformation, (ii) the amide planes rotate ca. 60° off the plane defined by the methylene carbons, and (iii) a chain packing close to hexagonal with diffraction spacings near 4.15 Å is found.

Although experimental evidences on a structure similar to the α form have been reported³ for some odd–even nylons, no alternative structure compatible with a complete hydrogen-bonding scheme has been suggested. However, we have recently reported a new structure for even–odd nylons derived from glutaric acid,^{4,5} where all hydrogen bonds can be satisfied. In this case they are established according to the two directions originated by the rotation on opposite senses of consecutive amide groups from the plane defined by the methylene carbons of the odd segment (Figure 1).

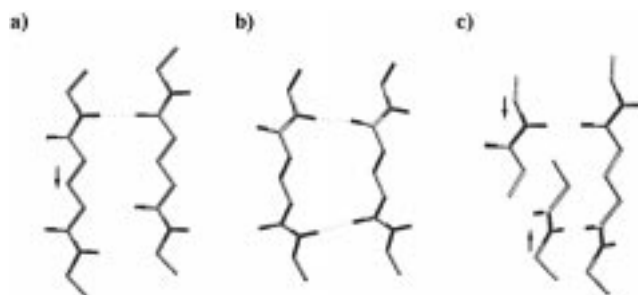


Figure 1. Possible models of n,m nylons when n is odd and m is even. (a) When the chains have an all-trans conformation all the amide planes point in the same direction. Thus, only 50% of the hydrogen bonds can be established with optimal geometry by a translation of neighbor molecules. (b) In the γ conformation postulated by Kinoshita,² the amide planes are tilted by 30° to the chain axis, allowing the formation of linear hydrogen bonds between parallel molecular chains. (c) A good hydrogen bond system, in two directions, can also be produced when the amide planes slightly deviate in opposite senses from the plane defined by the methylene carbons of the diamine. Note that in this case the neighboring chains are at different heights. Arrows indicate the shift direction of the chains with respect to the unlabeled one. To simplify the figures, only selected fragments and hydrogen atoms of amide groups have been represented.

A related structure has also recently been postulated by Franco et al. for nylon 6,9,⁶ showing that it is independent of the odd dicarboxylic residue length.

In a recent work on nylon 9,2,⁷ where only one polymethylene segment exists in the structural unit, we started the study of odd–even nylons. There, we concluded that the new structure with two hydrogen bond directions may be also present on nylons derived from odd diamines. We have also emphasized the close resemblance between the conventional α phase and this new structure. In this paper we present a structural study of an odd–even nylon which has polymethylene segments in both diamine and diacid units. We have selected nylon 5,6, first because it is an isomeric compound of the previously studied nylon 6,5⁴ and second because it is close to nylon 6,6, one of the most

studied nylons owing to its commercial applications. Up to the present time, diffraction data on nylon 5,6 are scarce. Dreyfuss⁸ prepared single crystal mats of nylon 5,6, but only a lamellar long spacing of 56 Å and chain repeat spacings of 14.1 and 7.05 Å were reported. Magill³ determined from spherulitic crystallization studies, the existence of two crystalline forms. Thus, a γ form (with X-ray diffraction spacings at 7.2–7.1, 4.18, and 4.05 Å) was predominant after melt crystallization, although spacings attributed to an α phase (4.35 and 3.8 Å) were also detected.

Experimental Section

Synthesis and Characterization. Nylon 5,6 was synthesized by interfacial polycondensation of 1,5-diaminepentane and adipoyl dichloride, in a manner similar to that reported for nylon 6,5.⁴ Approximately 30 mmol of the dichloride dissolved in 150 mL of toluene was added dropwise to a solution of 30 mmol of the diamine and 120 mmol of NaOH in 150 mL of water. The polyamide film produced in the interface of the two solutions was slowly pulled out of the beaker in a continuous fashion. The resulting ropelike polymer was successively washed with water, ethanol, toluene, and ethyl ether before drying in a vacuum desiccator at 60 °C.

The intrinsic viscosity of the polymer was determined with a Cannon-Ubbelohde microviscometer in dichloroacetic acid solutions at 25 ± 0.1 °C. The infrared absorption spectrum was recorded from potassium bromide pellets with a Perkin-Elmer 783 spectrophotometer in the 4000–500 cm^{-1} range. NMR spectra were registered from polymer solutions in deuterated trifluoroacetic acid, using tetramethylsilane (TMS) as an internal standard. A Bruker AMX-300 spectrometer operating at 300.1 and 75.5 MHz was used for ^1H NMR and ^{13}C NMR investigations, respectively. Thermal behavior was investigated with a Perkin-Elmer DSC-4 at a heating rate of 10 °C/min in a nitrogen atmosphere. The instrument was calibrated for temperature and heat of fusion using an indium standard.

Structural Methods. Spherulites were grown from melt-crystallized thin films, which were produced by heating small amounts of polymer on microscope slides. These films were crystallized isothermally using a Mettler FP80 thermal analysis system instrument. Morphologies were observed by polarizing optical microscopes (Nikon Microflex AFX-DX and Carl Zeiss Standard GFL). A first-order red tint plate was adopted to determine the sign of spherulite birefringence under cross-polarization.

Crystallization experiments were carried out isothermally from dilute solutions (0.05–0.1% (w/v)) in polar polyfunctional alcohols such as 1,4-butanediol, 2-methyl-2,4-pentanediol, and glycerine. The polymer was dissolved at 210 °C and the solution was transferred to constant-temperature baths in the 70–165 °C interval for 2–5 h. Crystallization experiments were also carried out from dilute solutions of the polymer in different mixtures of formic acid and ethanol at temperatures between 25 and 70 °C. For electron microscopy the crystals were deposited on carbon coated grids which were then shadowed with Pt–carbon at an angle of 15°. A Philips EM-301 electron microscope operating at either 80 or 100 kV for bright field and electron diffraction modes, respectively, was used throughout this work. Electron diffraction patterns were recorded by the selected area method on Kodak Tri-X films. The patterns were internally calibrated with gold ($d_{111} = 2.35$ Å).

X-ray diagrams were recorded under vacuum at room temperature, and calcite ($d_B = 3.035$ Å) was used for calibration. A modified Statton camera (W. R. Warhus, Wilmington, DE) with Ni-filtered copper radiation of wavelength 1.542 Å was used for these experiments. Patterns were recorded from either polymer powders, fibers, or mats of single crystals, which were prepared by slow filtration of a crystal suspension through a glass filter. Fiber patterns were also registered as

a function of temperature by using a temperature-controlled chamber provided by the manufacturer.

Structural modeling was carried out by using the software package CERIUS 3.1.⁹ Standard bond lengths and angles for polyamides were adopted to build the repeating unit and were fixed throughout the whole modeling process. Furthermore, only the four torsion angles next to the amide groups were allowed to vary from 180°. Peaks in the simulated fiber diffraction patterns were broadened with a Lorentzian profile and a disorientation angle was introduced in order to reproduce the arched reflections. Polarization and temperature ($B = 10$ Å²) factors were included in calculations that were run on a Silicon Graphics Indigo Workstation.

Energy Calculations on the α -Like Phase. Energy calculations were performed in all cases using quantum mechanical methods. Conformational energies for an isolated polymer chain were computed using a model compound constituted by two repeat units, which were blocked at the ends by acetyl and *N*-methanamide terminal groups. Atomic coordinates for the different conformations were taken from the models built with the CERIUS program. Thus, single point energy evaluations were performed on the selected conformations at the *ab initio* HF/3-21G¹⁰ and HF/6-31(d)¹¹ levels, as well as at the semiempirical INDO¹² and AM1¹³ levels.

The relative stability between selected crystal structures was estimated at the semiempirical AM1 level. For comparison purposes primitive unit cells were considered in all cases. Thus, the studied systems consist of four chains, each one constituted by one repeat unit blocked at the ends by the previously indicated terminal groups.

Results and Discussion

Synthesis and Characterization. Interfacial polymerization gives nylon 5,6 in a 47% yield and an intrinsic viscosity of 0.63 dL/g (measured in dichloroacetic acid at 25 °C), which was in agreement with the film and fiber forming properties of the polymer. The infrared spectrum showed characteristic amide and methylene absorption bands: 3308 (amide A), 3078 (amide B), 2938 and 2862 (C–H), 1636 (amide I), 1542 (amide II), 688 (amide V), and 578 cm^{-1} (amide VI). Furthermore, no signals of terminal groups or irregularities were detected in the NMR spectra: ^1H NMR (300.1 MHz, TFA-*d*) δ 1.50 (2H, $\text{NHCH}_2\text{CH}_2\text{CH}_2$), 1.78 (4H, NHCH_2CH_2), 1.93 (4H, COCH_2CH_2), 2.72 (4H, COCH_2), 3.57 (4H, NHCH_2); ^{13}C NMR (75.7 MHz, TFA-*d*) δ 24.64 (COCH_2CH_2), 26.01 ($\text{NHCH}_2\text{CH}_2\text{CH}_2$), 28.49 (NHCH_2CH_2), 34.36 (COCH_2), 43.38 (NHCH_2), 179.82 (CONH).

Two melting peaks at 220 (broad and low) and 250 °C were found in the calorimetric analysis. These values are close to the data previously reported¹⁴ for nylon 5,6 (223–225 and 251–258 °C) and compare well with the data found in the isomer compound: nylon 6,5⁴ (230–234 and 240–243 °C). The DSC studies showed also that the polymer was stable through fusion, since the transitions observed on heating were reproducible after a cooling run from the melt. A crystallinity around 52% could be evaluated taking into account the total heat of fusion (20.95 kJ/mol) and the equilibrium heat of fusion (40 kJ/mol) calculated from the reported¹⁵ group contributions of the amide and methylene groups.

Structural Data for the α -Like Phase. Nylon 5,6 shows polymorphism depending on the conditions of sample preparation. Thus, a structure with the most intense diffraction signals (4.32 and 3.75 Å) close to the characteristic spacings of an α -form can be obtained from (a) samples coming directly from interfacial polymerization (Figure 2a), (b) Annealed fibers prepared

Table 1. Measured and Calculated X-ray and Electron Diffraction Spacings d_B (Å) for Different Nylon 5,6 Samples in the α -Like Form: Powder Recovered from Synthesis, Annealed Fiber at 140 °C, Mat of Sedimented Crystals Obtained from a Formic Acid–Ethanol (1:4) Solution, and Lamellar Crystal from the Same Crystallization Conditions

index ^a	calcd	powder ^{b,c}	fiber ^{b,c}	crystal mat ^{b,c}	single crystal ^{b,d}
lamellar thickness	54			54 s ^f	
second order lamellar thickness	27			27 w	
002	12.72	14.0–12.5 w	12.7 w, off M	12.7 vw	
004	6.36	6.36 s	6.36 s, off M	6.36 s	
020	4.32	4.32 vs	4.32 vs, E	4.32 vs	4.32 vs
110	3.75	3.75 vs	3.75 vs, E	3.75 vs	3.75 ^e s
111	3.45	3.43 w	3.43 m, off M	3.44 w	
119	3.21		3.24 m, off M		
008	3.18		3.14 m, off M		
11 $\bar{1}$ 2	2.49		2.44 w, M		
131, 130	2.43, 2.37		2.39 m, E		–, 2.39 ^e w
11 $\bar{1}$ 3	2.30		2.29 s, M		
139	2.21		2.20 w, off M		
040	2.16				2.16 w
22 $\bar{1}$ 2	2.03		2.06 w, off M		
13 $\bar{1}$ 2	1.93		1.92 w, off M		

^a On the basis of a centered monoclinic cell: $a = 5.12$ Å, $b = 8.64$ Å, c (chain axis) = 31.33 Å, and $\beta = 125.7^\circ$. ^b Abbreviations denote intensities or orientation: vs, very strong; s, strong; m, medium; w, weak; M, meridional; E, equatorial; off M, off meridional. ^c X-ray diffraction data. ^d Electron diffraction data. ^e The equivalent $hk0$ reflections have also been observed. ^f Observed only in the low-angle X-ray patterns.

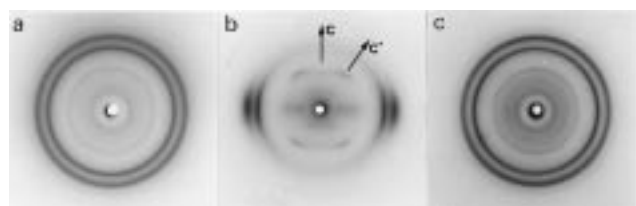


Figure 2. (a) Powder pattern of nylon 5,6 coming directly from interfacial polymerization. (b) X-ray fiber pattern of nylon 5,6 annealed at 140 °C. The fiber was kept under stress during exposure, to improve the quality of the pattern, since some elastic behavior was observed. (c) Mat of sedimented crystals obtained from formic acid–ethanol (1:4) mixtures. Only a slight orientation is detected in the characteristic rings at 4.32 and 3.75 Å.

from the melt (Figure 2b), and (c) single crystals obtained from crystallizations carried out in formic acid–ethanol (1:4) mixtures (Figures 2c and 3). This form can also be obtained, but not exclusively, in crystallizations from polyfunctional alcohols where the crystallization temperature was higher.

Table 1 summarizes all the reflections found in the different X-ray and electron diffraction patterns and shows also their indexing according to a centered monoclinic unit cell of parameters: $a = 5.12$ Å, $b = 8.64$ Å, c (chain axis) = 31.33 Å, and $\beta = 125.7^\circ$. Although this unit cell can be reduced to a primitive triclinic cell ($a = 5.12$ Å, $b = 5.02$ Å, c (chain axis) = 31.33 Å, $\alpha = 107.4^\circ$, $\beta = 125.7^\circ$, and $\gamma = 59.3^\circ$), we disregarded this possibility taking into account symmetry considerations, as it will be discussed below. Note also that the electron diffraction pattern is consistent with a rectangular cell of 4.16×8.64 Å² where both diagonals form an angle of 51.4° and are equal to twice the characteristic 4.79 Å distance between hydrogen-bonded chains. This projection is similar to the 4.20×8.62 Å² reported for nylon 6,⁵⁴ and slightly deviates from the alternative rectangular cell reported by Bunn and Garner¹ for nylon 6,6 (4.03×8.73 Å²). In any case the experimental evidences are close to those reported for nylon 6,⁵⁴ where the centered unit cell was justified according to both the mm symmetry and the systematic absences found in the electron diffraction patterns. Unfortunately, the lamellar crystals of nylon 5,6 were very narrow (0.1 μ m), and

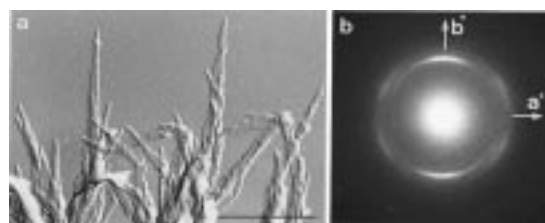
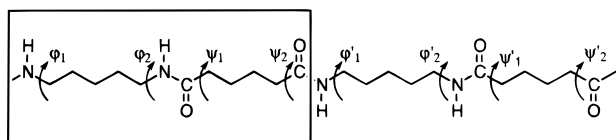


Figure 3. (a) Transmission electron micrographs of nylon 5,6 obtained from formic acid–ethanol (1:4) solutions at 78 °C. Crystals have a lath-shaped morphology with very irregular edges. A thickness around 60 Å can be estimated from their shadow in the micrographs (scale bar 1 μ m). (b) Electron diffraction pattern of the lamellar crystals. Note the sharpness of the 020 reflection with respect to the diffuse 110 and $\bar{1}\bar{1}0$ reflections. The orientation of the pattern is such that b^* corresponds to the long axis of the single crystals.

consequently few reflections were observed in their diffraction pattern (Figure 3b). Despite this, an mm symmetry is consistent with the reflections observed. In all cases the diffraction signals were arched, indicating that the patterns arise from a group of crystals with similar orientations, as the multilayered lath-shaped lamellae depicted in Figure 3a. Note also that the 3.75 Å (110 and $\bar{1}\bar{1}0$) reflections appear broad and diffuse in contrast with the inner one at 4.32 Å (020). This fact may be justified by the tilting of the molecular chains with respect to the lamellar surface (ab face), as expected from the monoclinic unit cell with $\beta \neq 90^\circ$. Although the mat of sedimented crystals (Figure 2b) has a very poor orientation (probably owing to the small dimensions of the elongated lamellae), a different orientation can be detected between the 020 reflection (maximum intensity of the ring in the equator) and the 110 reflection (off equatorial orientation). This difference gives support to the idea that the molecular chains are tilted in the way previously indicated.

The tilting can be measured in the fiber diffraction pattern (cc^* angle, Figure 2c) and corresponds to ca. 36° . On the other hand, from the layer lines observed in the fiber pattern a value of 31.33 Å for the chain axis parameter can be determined. This value deviates from that expected for an extended conformation (31.82 Å) and consequently indicates that some torsion angles differ from 180° .

Scheme 1



The space group of nylon 5,6 is expected to have a c glide plane, since only the $00l$ reflections with $l = \text{even}$ can be observed in the X-ray diffraction patterns. Note that a 2-fold screw axis in the c (chain axis) direction has to be rejected, since β is the monoclinic angle of the unit cell. Moreover, the molecular symmetry should have additional symmetry operators (i.e., binary axis, center of symmetry, or mirror plane), which have to relate the halves of both diamine and diacid units in order to comply with the equivalence postulate of Natta and Corradini.¹⁶ If those symmetry elements were preserved in the space group, the crystal is expected to have a $C12/c1$ symmetry. Note that in this case the m mirror plane is not possible, since an orthorhombic unit cell is derived, taking into account the existence of the c glide plane. On the other hand the selected space group together with the cell dimensions indicate that hydrogen bonds must be established along both diagonals of the centered unit cell. A single hydrogen bond system would imply that the symmetry were reduced to $P1$, since both diagonals are then not equivalent. Thus, the systematic absences and the symmetry of the diffraction patterns are not well explained in a $P1$ space group.

The interlamellar stacking periodicity was measured as 54 Å in the low angle X-ray diffraction pattern and corresponds to approximately 3.5 structural units. Thus, the folds at either side of the lamellae probably show some degree of disorder, as indicated by the noninteger number of chain units in the lamellae.

Structural Modeling of the α -Like Phase. The modeling of a structure compatible with geometrical constraints (chain repeat length, packing and hydrogen bond geometry) and diffraction data (from fibers and single crystals) was carried out varying the torsion angles φ_i and ψ_i of the diamine and diacid units (Scheme 1), respectively. Relationships due to the molecular symmetry requirements ($2/c$) were also imposed. Thus, due to the presence of a glide plane, the torsion angles of consecutive units (i.e., φ_1 and φ'_1 or ψ_1 and ψ'_1) must be equal but with opposite signs. Furthermore, a binary axis perpendicular to the molecular chain through the middle of the diamine unit and an inversion center in the middle of the dicarbonyl unit require $\varphi_1 = \varphi_2$ and $\psi_1 = -\psi_2$, respectively. Although symmetry considerations point to a system with two hydrogen bond directions, we have also considered the possibility of a single direction. Thus, molecules have been oriented in the unit cell in order to establish hydrogen bonds along the two diagonals or along the b axis for the centered or primitive unit cell, respectively.

The rotation angle (τ) defined by the two N-H directions of the $-\text{CONH}(\text{CH}_2)_5\text{NHCO}-$ segment depends on the torsion angles φ_i , as shown in Figure 4a. A system with a single hydrogen bond direction is derived for $\tau = 0^\circ$ (case 1) or 180° (case 2), which correspond to $\varphi_1 = 180$ or 70° , respectively. Amide groups progressively deviate in opposite senses from the plane defined by the diamine carbons, when both φ_1 and φ_2 angles decrease from 180° . Thus, a rotation angle τ

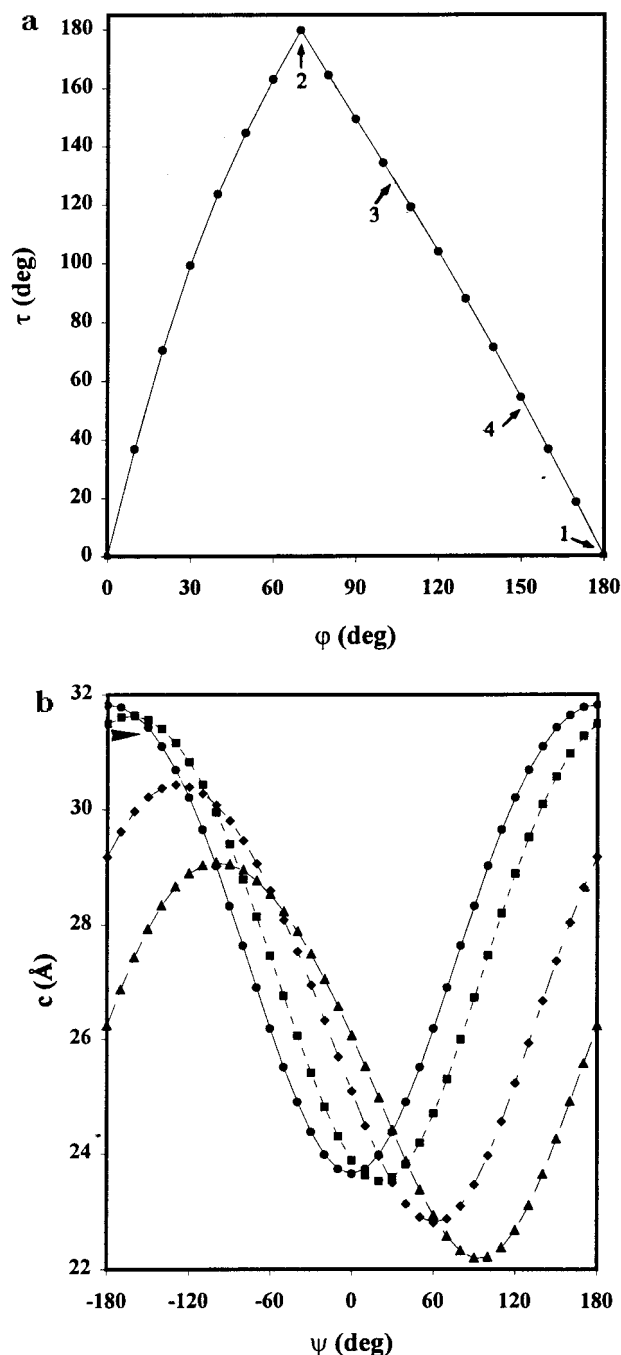


Figure 4. (a) Calculated rotation angle (τ) between the two NH directions of the diamine moiety for different $\varphi_1 = \varphi_2$ torsion angles. Arrows indicate selected geometries with $\tau = 0$ (1), 52 (4), 128 (3), and 180° (2). (b) Calculated chain repeat length as a function of the torsion angle ψ_1 for selected φ_1 values. Arrow indicates the observed chain repeat value. In all cases a $2/c$ molecular symmetry has been considered. (●) case 1, $\varphi_1 = \varphi_2 = 180^\circ$; (▲) case 2, $\varphi_1 = \varphi_2 = 70^\circ$; (◆) case 3, $\varphi_1 = \varphi_2 = 104^\circ$; (■) case 4, $\varphi_1 = \varphi_2 = 152^\circ$.

of 128 or 52° is obtained for $\varphi_1 = 104$ (case 3) or 152° (case 4), respectively. These two values correspond to a two-hydrogen-bonding system compatible with the dimensions of the projected monoclinic unit cell. On the other hand the ψ_1 dependence on the chain repeat length (c) is shown in Figure 4b for the indicated cases.

Case 1. Its conformation ($\varphi_1 = \varphi_2 = 180^\circ$ and $\psi_1 = -\psi_2 = 147^\circ$) approaches the all-trans conformation characteristic for an α structure. The deviation of the ψ_i angles accounts for the experimental shortening of

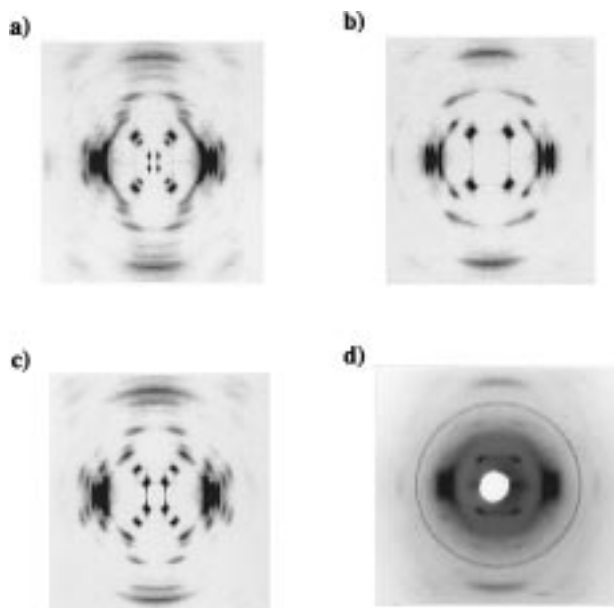


Figure 5. Experimental and simulated⁹ X-ray diffraction fiber patterns: (a) case 1; (b) case 4, model 1; (c) case 4, model 2. All patterns have been simulated using identical parameters (crystal size, temperature factor, and degree of arcing). For comparative purposes the experimental pattern is given in part d. Note the relatively good agreement between parts b and d.

the chain repeat unit (0.12 Å/amide group). Two reasons allow us to discard this model: (i) the bad hydrogen bond geometry, since half of the amide interactions are characterized by $d_{\text{H}\cdots\text{O}} > 3.7$ Å, and (ii) the single hydrogen bond direction, which implies a primitive unit cell and a $P1$ space group, which as previously discussed is in disagreement with the diffraction data. Note also that the relatively high intensity of the 001 and 003 reflections in the simulated X-ray fiber diffraction pattern (Figure 5a) does not compare at all with the experimental pattern.

Case 2. The hydrogen bond geometry can be improved when $\varphi_1 = \varphi_2 = 70^\circ$ and the neighboring chains are conveniently shifted. However, as shown in Figure 4b, the expected chain repeat length is always much shorter than the experimental one.

Case 3. A conformation with $\varphi_1 = \varphi_2 = 104^\circ$ can also be rejected, since (i) the binary axis has to be parallel to the a direction of the centered unit cell, which is in disagreement with $\beta \neq 90^\circ$, and (ii) the calculated chain repeat length (Figure 4b) is also always lower than the experimental one.

Case 4. When $\varphi_1 = \varphi_2 = 152^\circ$, two conformations appear compatible with a chain repeat length of 31.33 Å. These values correspond to $\psi_1 = -\psi_2 = -137^\circ$ (model 1) and $\psi_1 = -\psi_2 = 175^\circ$ (model 2). Although the hydrogen bond geometry is similar (model 1, $d_{\text{H}\cdots\text{O}} = 2.00$ Å, $d_{\text{N}\cdots\text{O}} = 3.00$ Å, and $\angle\text{NH}\cdots\text{O} = 170^\circ$; model 2, $d_{\text{H}\cdots\text{O}} = 2.09$ Å, $d_{\text{N}\cdots\text{O}} = 3.08$ Å, and $\angle\text{NH}\cdots\text{O} = 165^\circ$), the simulated fiber diffraction pattern of model 1 (Figure 5b) is closer to the experimental data than in the case of model 2 (Figure 5c). Note in particular the different intensities of the 00/ l reflections.

The model presented here for nylon 5,6 is very similar to that previously reported for nylon 6,5.⁴ Thus, the even moiety adopts in both cases an s^-t_4s conformation, whereas the odd unit is characterized by torsion angles close to 150° for the bonds adjacent to the amide groups.

The calculated electron diffraction pattern for single crystals has 110 and $1\bar{1}0$ reflections more intense than

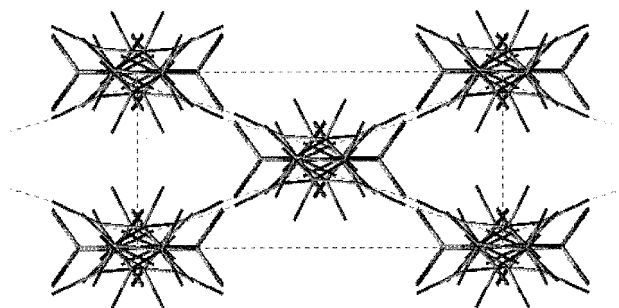


Figure 6. Equatorial projection of the centered unit cell for the model proposed for nylon 5,6. Note that hydrogen bonds (dashed lines) are established along both diagonals.

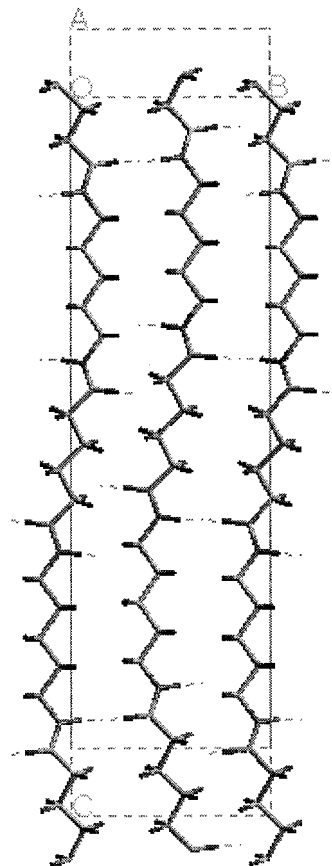


Figure 7. bc projection of the unit cell for the proposed model. The central molecular chain is at a different level in the a direction. Note also that the relative displacements in the c direction (approximately one bond) improves the hydrogen bond geometry.

the 020 reflection. The reduced lamellar thickness and the high intensity of the 110/110 reflections explain why they are still present (broad and diffuse) in the experimental patterns (Figure 3b), although these planes are tilted with respect to the electron beam.

Molecular drawings of equatorial and lateral projections for the final molecular arrangement (model 1) are shown in Figures 6 and 7, respectively.

Energy Calculations on the α -Like Phase. Calculations have been carried out in order to compare the postulated model 1 with the structure based on the characteristic all-trans conformation of nylons. Thus, we have built two theoretical new models (3 and 4), which of course have a chain axis parameter slightly larger than the experimental one. Model 3 is based on the molecular packing of nylon 6,6¹⁴ and so the unit cell

Table 2. Conformational Energies (kcal/mol) for an Isolated Chain of a Nylon 5,6 Model Compound

computational level	model 1	models 3 and 4
INDO	0.0	1.2
AM1	0.0	0.9
HF/3-21G	0.0	2.1
HF/6-31(d)	0.0	0.8

has the same parameters except for that corresponding to the chain axis ($a = 4.90$ Å, $b = 5.40$ Å, $c = 31.82$ Å, $\alpha = 48.5^\circ$, $\beta = 77^\circ$, and $\gamma = 63.5^\circ$). Note that, as in nylon 6,6, the molecular chains are shifted within the sheets ($\beta = 77^\circ$). However, in this case only half of the amide groups (Figure 1b) have a good hydrogen bond geometry ($d_{H\cdots O} = 2.14$ Å, $d_{N\cdots O} = 3.08$ Å, and $\angle NH\cdots O = 154^\circ$ with respect to $d_{H\cdots O} = 3.44$ Å, $d_{N\cdots O} = 3.99$ Å, and $\angle NH\cdots O = 116^\circ$). Model 4 ($a = 4.77$ Å, $b = 5.40$ Å, $c = 31.82$ Å, $\alpha = 48.5^\circ$, $\beta = 90^\circ$ and $\gamma = 72.3^\circ$) corresponds to a modification where shearing of chains within the sheets has been eliminated ($\beta = 90^\circ$). Thus, all hydrogen bonds are equivalent ($d_{H\cdots O} = 2.65$ Å, $d_{N\cdots O} = 3.39$ Å, and $\angle NH\cdots O = 130^\circ$), but with a poor geometry.

Conformational energies computed for an isolated chain of a model compound are listed in Table 2. Note that the energies were only computed for two different conformations, which were the shortened structure of model 1 and the fully extended conformation of models 3 and 4. The shortened conformation was energetically favored with respect to the fully extended one independently of the level of the theory. Thus, the relative energy between the two conformations varies from 0.8 kcal/mol at the HF/6-31(d) level to 2.12 kcal/mol at the HF/3-21G level. This result is in agreement with those obtained in a rotational profile of the bonds next to the amide groups specifically computed for nylons.¹⁷ Thus, the values of the dihedral angles for the shortened conformation are close to the position of the minimum of such profiles than the values of the fully extended one.

The relative stability of the different models was also investigated using semiempirical quantum mechanical calculations. An inspection to the results displayed in Table 2 indicates a good agreement between *ab initio* HF/6-31(d) and AM1 energies for this molecular system. Furthermore, the semiempirical AM1 method provides a reasonable description of the intermolecular hydrogen bonds.¹⁸ AM1 calculations were performed on the triclinic unit cells of models 3 and 4 and the equivalent cell of model 1. Thus, the three systems have the same number of stacking interactions between methylene groups. However, model 1 has one amide–amide interaction less than models 3 and 4. Therefore the stability of the former will be underestimated by quantum mechanical calculations.

As was expected, the structure with two hydrogen bond directions (model 1) was found to be energetically favored with respect to the models based on the all-trans conformation, having a single hydrogen bond direction. Thus, models 3 and 4 were unfavored by 5.7 and 8.9 kcal/mol, respectively, despite considering one more amide–amide interaction. In conclusion, model 1 is stabilized from a conformational point of view (see Table 2), also taking into account the intermolecular interactions.

Structural Data on the γ Form. A second structure, which is related to the γ form can also be obtained when the preparation conditions are changed. Thus,

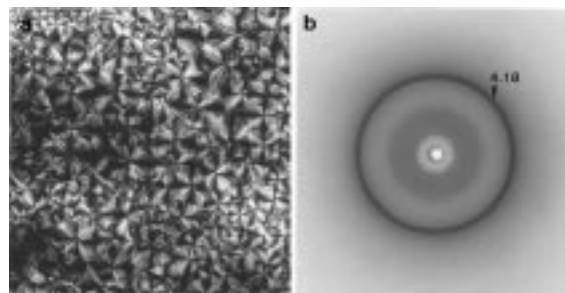


Figure 8. (a) Positively birefringent spherulites grown at 200 °C, after melting nylon 5,6 at 255 °C. A fibrillar-looking appearance is characteristic, in agreement with the melt crystallization studies of Magill.³ (b) Powder X-ray diffraction pattern of nylon 5,6 spherulites. The high-intensity ring at 4.18 Å is indicative of a γ -phase, as it was previously reported by Magill.³

crystallization from the melt renders positive spherulites (Figure 8a). Their X-ray powder diffraction pattern is characterized by a strong reflection at 4.18 Å (Figure 8b). In addition to this chain packing spacing, some broad and diffuse rings attributed to the chain repeat can also be observed (Table 3).

A pseudohexagonal form is also characteristic of fibers obtained from the melt without further processing (Figure 9a). However, when these fibers are annealed under stress, the α -like phase also appears. Figures 9b,c and 2b show different proportions of the two phases, depending on the annealing treatment (time and stress). Note that the 004 reflections of both structures can be well differentiated (off meridional and meridional orientations for the α -like and γ phase, respectively).

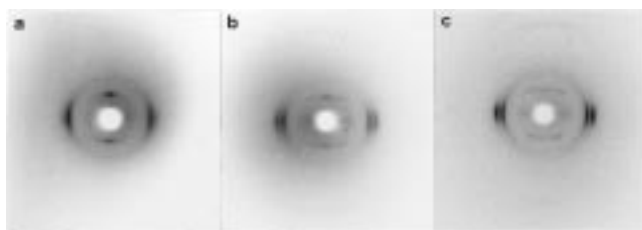
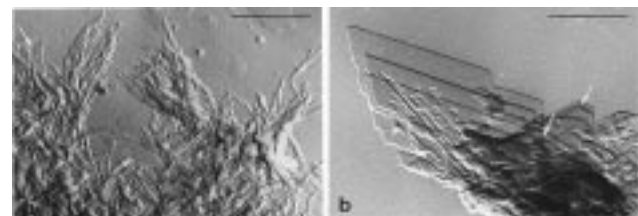
Lamellar crystals of the γ form can also be obtained, together with the α -like form, from crystallizations in polyfunctional alcohol solutions. Figure 10a shows a multilamellar aggregate of crystals belonging to the γ form. Note that the individual lamellae have very irregular edges and dimensions. In general these single crystals do not have the lath-shaped morphology displayed for the α -like lamellae, since they are wider and even an incipient lozenge habit is found (Figure 10a). This morphology is more apparent in the crystals prepared in glycerine at 140 °C (Figure 10b) from a low molecular weight sample. In this case, angles around 120 °C can be measured between their edges. Note also that both regular and irregular edges are present in the same lamella.

Figure 11 shows the electron diffraction pattern from one of these crystals. It is characterized by the fact that two (4.12 Å) of the six inner spots appear at slightly different spacings than the other four (4.20 Å). Thus, it is clear that the unit cell deviates from hexagonal. In addition, the intensities of the reflections indicate that the symmetry of the pattern is even lower than *mm* (i.e., 200 vs 220). This fact is usually expected for a γ form, where a single hydrogen bond direction exists. A tentative unit cell with parameters $a = 4.88$ Å, $b = 4.79$ Å, $c = 28.8$ Å, and $\gamma = 59.3^\circ$ can be derived from the X-ray and electron diffraction data (Table 3). Note that the b parameter coincides with the characteristic distance between hydrogen-bonded chains and a shortening of ca. 0.75 Å/amide group with respect to the all-trans conformation can be derived. Thus, nylon 5,6 may have some distortion from the γ conformation, since this shortening is higher than the reported value¹⁹ (0.35 Å/amide). Moreover the weak 003 reflection found in the powder pattern suggests a deviation of the expected

Table 3. Measured and Calculated X-ray and Electron Diffraction Spacings d_B (Å) for Different Nylon 5,6 Samples in the γ Form: Spherulites Crystallized from the Melt at 200 °C, Fibers Obtained from the Melt, and Lamellar Crystals Prepared from Glycerine (0.1 w/v) at 142 °C

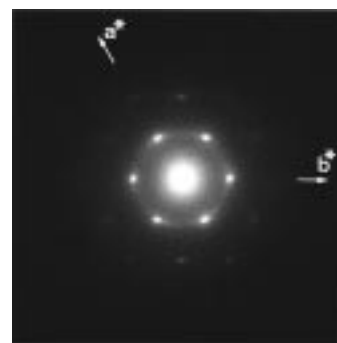
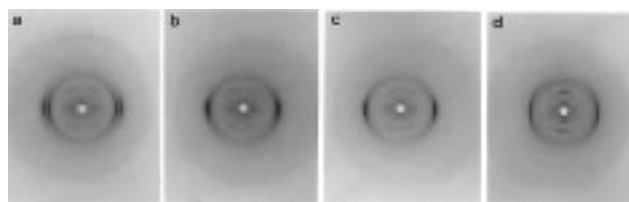
index ^a	calcd	spherulitic sample ^{b,c}	fiber ^{b,c}	single crystal ^{b,d}
002	14.40	14.4 m	14.3 w M	
003	9.60	9.60 vw		
004	7.20	7.20 m	7.10 m M	
100, 110, 010	4.20, 4.20, 4.12	4.18 vs	4.18 vs E	4.20 vs, 4.20 vs, 4.12 vs
103, 113, 013	3.85, 3.85, 3.79	3.82 vw	3.82 w	
210	2.44			2.43 s
200	2.10			2.10 m
220	2.10			2.10 w
120	2.39			2.39 w
110	2.39			2.39 w
020	2.06			2.06 vw
320	1.60			1.60 vw
310	1.60			1.60 vw

^a On the basis of a centered monoclinic cell: $a = 4.88$ Å, $b = 4.79$ Å, c (chain axis) = 28.80 Å, and $\beta = 59.3^\circ$. ^b Abbreviations denote intensities or orientation: vs, very strong; s, strong; m, medium; w, weak, vw, very weak; M, meridional; E, equatorial. ^c X-ray diffraction data. ^d Electron diffraction data.

**Figure 9.** (a) X-ray pattern of a fiber in the γ form obtained from the melt. The most intense reflections correspond to 7.20 and 4.18 Å spacings and appear oriented on the meridian and on the equator, respectively. (b and c) X-ray fiber patterns of samples with different proportions of γ - and α -like crystalline structures.**Figure 10.** (a) Single crystals of nylon 5,6 in the γ form obtained from 2-methyl-2,4-pentanediol at 140 °C. Arrows point to the crystals with greater lateral dimensions. (b) Lamellar crystals obtained in glycerine at 140 °C. The polymer used in this case corresponds to a sample with an intrinsic viscosity of 0.31 dL/g. Arrows indicate angles close to 120° (scale bars 1 μ m).

$2_1/m$ molecular symmetry for an odd-even nylon in a γ conformation.

Brill Transition. Changes in the fiber X-ray diffraction pattern of a sample in an initial α -like phase have been studied from 25 to 220 °C. In Figure 12 are presented representative patterns which show a significant variation in spacings and consequently in the lattice parameters as a function of temperature, as is found in other polyamides. Thus, the equatorial reflections (4.32 and 3.75 Å) gradually merge into a single one at 4.23 Å, just below 220 °C (Figure 13a) in the so-called "Brill" transition temperature. Although a great number of studies have been reported for different nylons,^{6,20–36} a complete understanding of this behavior does not yet exist. Thus, different explanations have been given: (i) the anisotropy of the thermal expansion;²⁰ (ii) a development of a three-dimensional network of hydrogen bonds giving a pseudohexagonal unit cell;^{6,21–23} (iii) a transition that involves different pro-

**Figure 11.** Selected area electron diffraction pattern of nylon 5,6 crystals in the γ form obtained from glycerine at 140 °C. The sample was characterized by an intrinsic viscosity of 0.6 dL/g.**Figure 12.** Influence of the temperature on the X-ray diffraction patterns of an annealed fiber of nylon 5,6. The patterns were taken at the following temperatures: (a) 50 °C; (b) 160 °C; (c) 190 °C; (d) 220 °C.

portions of two unique phases, the low temperature and a second one, which justify the pseudohexagonal arrangement, taking into account the librational motion of methylene groups at high temperature.²⁶ In this sense the evolution of the 004 reflection (Figure 13b) appears to be highly relevant, since both spacing and cc^* angle gradually change in the 25–190 °C interval, in a manner similar to that previously reported for nylon 6,5. Note that this behavior is clearly different from that reported in Figure 9 where different proportions of two structures (γ and α -like phases) give always distinguishable 004 reflections. We think this is an indication of a continuous change of the structure with temperature. For instance a slight distortion of the φ_i torsion angles (from 152° to 147°) may produce a 60° rotation angle (τ) between the NH directions of the diaminopentane units. This explanation is in agreement with the NMR observations^{27,28} on other nylons, where it was demonstrated that hydrogen bonds remain unchanged at high temperature. At 220 °C we have

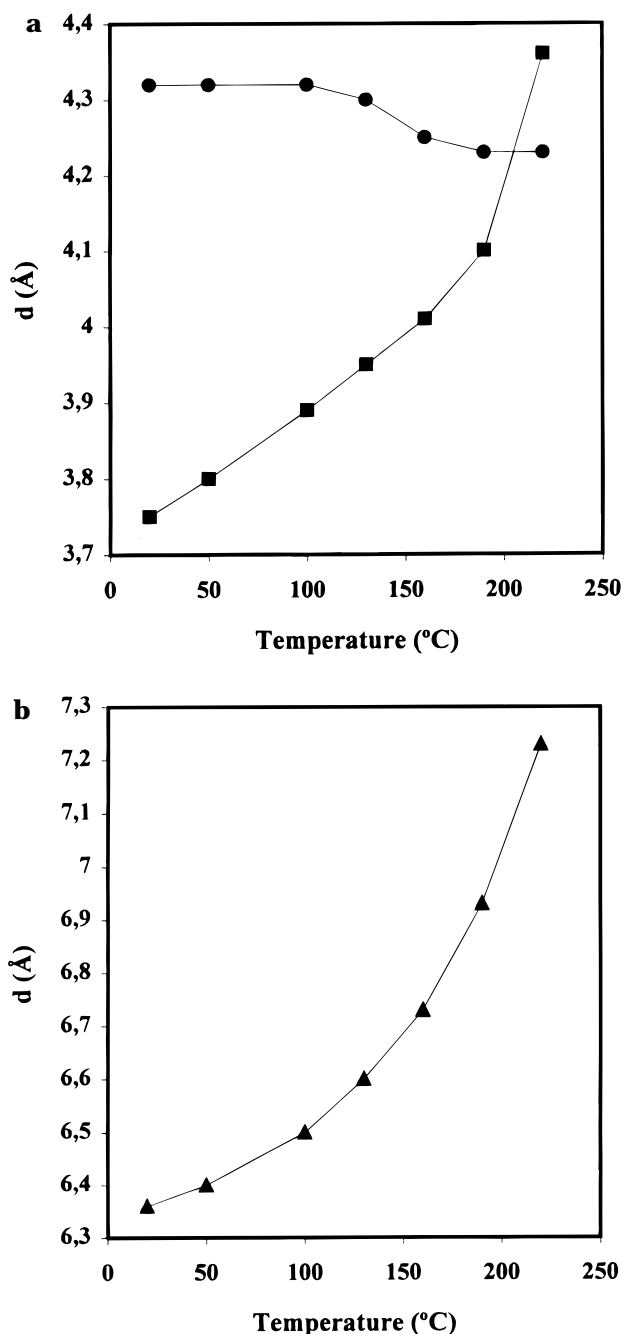


Figure 13. Plots showing the variation in: (a) equatorial (020) (●) and 110/110 (■) and (b) 004 chain repeat spacings, as nylon 5,6 fibers are heated from room temperature to 220 °C.

obtained a peculiar diffraction pattern where additional reflections at 4.54 and 4.36 Å appear and a meridional orientation is observed for the 004 reflection (Figure 12d). Note that this pattern is clearly different to that found in the low temperature γ form. Despite the small number of reflections and the indicated orientation for 004, we give a tentative monoclinic unit cell with $\beta \approx 90^\circ$ (Table 4). In fact, the disorientation and the reduced cc^* angle may justify the meridional appearance. Moreover a monoclinic unit cell seems to be the only way to index the 4.54 reflection without increasing the size of the unit cell. Note that the high temperature unit cell is related to that found at room temperature (Table 1), assuming a slight change in the angle between the two hydrogen bond directions and an increase in the packing parameters probably due to thermal expansion.

Table 4. Measured and Calculated X-ray Diffraction Spacings d_B (Å) for the High Temperature (220 °C) Structure of Nylon 5,6

index ^a	calcd	measd ^b
004	7.22	7.22 m
111	4.54	4.54 w
110	4.36	4.36 w
020	4.23	4.23 s

^a On the basis of a tentative monoclinic cell: $a = 5.51$ Å, $b = 8.46$ Å, $c = 31.33$ Å, and $\beta = 112.6^\circ$. ^b Abbreviations denote intensities: s, strong; m, medium; w, weak.

Conclusions

Our results show that nylon 5,6 may crystallize in two forms, one is the γ form and another corresponds to a structure with two hydrogen bond directions. They respectively crystallize in a monoclinic cell with the parameters $a = 4.88$ Å, $b = 4.79$ Å, c (chain axis) = 28.80 Å, and $\gamma = 59.3^\circ$ and a centered monoclinic cell with the parameters $a = 5.12$ Å, $b = 8.64$ Å, c (chain axis) = 31.33 Å, and $\beta = 125.7^\circ$. The latter form has reflections with similar spacings to those characteristic for the α structure of nylons, but the organization of hydrogen bonds is different. Simulations of the diffraction patterns and energy calculations indicate that an α structure, based on a fully extended conformation, is disfavored with respect to a model where hydrogen bonds are established according to two different directions. Structural data are fully consistent with a model where consecutive amide groups (those separated by the odd methylene segment) rotate in different senses from the plane defined by the methylene carbons. This model appears as an explanation for the α -like phase that is observed in both odd-even and even-odd nylons.

It appears therefore as a general feature of odd-even and even-odd nylons that they can have structures with two hydrogen bond directions, quite different from the conventional α and γ phases of polyamides. The conformational details found^{4-6,37} and the relative proportion of this structure and the γ form vary in each case.

Acknowledgment. This investigation has been supported by research grants from CICYT (MAT97-1013) and DGICYT (PB93-1067). L.F. acknowledges financial support from the Ministerio de Educación y Cultura. We are also thankful to J. L. Marcos for his help in experimental manipulations and to Dr. E. Navarro for her help in obtaining some of the fiber patterns reported here.

References and Notes

- (1) Bunn, C. W.; Garner, E. V. *Proc. R. Soc. London* **1947**, *189A*, 39.
- (2) Kinoshita, Y. *Makromol. Chem.* **1959**, *33*, 2 1.
- (3) Magill, J. H. *J. Polym. Sci., Polym. Phys. Ed.* **1973**, *11*, 201.
- (4) Navarro, E.; Franco, L.; Subirana, J. A.; Puiggali, J. *Macromolecules* **1995**, *28*, 8742.
- (5) Navarro, E.; Subirana, J. A.; Puiggali, J. *Polymer* **1997**, *38*, 3429.
- (6) Franco, L.; Cooper, S. J.; Atkins, E. D. T.; Hill, M. J.; Jones, N. A. *J. Polym. Sci., Polym. Phys. Ed.* **1998**, *36*, 1153.
- (7) Franco, L.; Subirana, J. A.; Puiggali, J. *Macromolecules*, in press.
- (8) Dreyfuss, P. *J. Polym. Sci., Polym. Phys. Ed.* **1973**, *11*, 201.
- (9) CERIUS 3.1 (Biosym/Molecular Simulations Inc.), Cambridge, U.K.
- (10) Binkley, J. S.; Pople, J. A.; Hehre, W. J. *J. Am. Chem. Soc.* **1980**, *102*, 939.
- (11) Hariharam, P. C.; Pople, J. A. *Theor. Chim. Acta* **1973**, *23*, 213.

- (12) Pople, J. A.; Beveridge, D. L.; Dobosh, P. A. *J. Chem. Phys.* **1967**, *47*, 2016.
- (13) Dewar, M. J. S.; Zoebisch, E. G.; Healy, E. F.; Steward, J. J. P. *J. Am. Chem. Soc.* **1985**, *107*, 3902.
- (14) Miller, R. L. *Polymer Handbook*, 3rd ed.; Brandrup, J., Immergut, E. H., Eds.; Wiley-Interscience: New York, 1989; Chapter VI.
- (15) Van Krevelen, D. W. *Properties of Polymers*, 3rd ed.; Elsevier: Amsterdam, 1990.
- (16) Natta, G.; Corradini, P. *Nuovo Cimento* **1960**, *15*, 9.
- (17) Bernadó, P.; Alemán, C.; Puiggali, J. Submitted work.
- (18) Alemán, C.; Navas, J. J.; Muñoz-Guerra, S. *J. Phys. Chem.* **1995**, *99*, 17653.
- (19) Kinoshita, Y. *Makromol. Chem.* **1959**, *35*, 1.
- (20) Holmes, D. R.; Bunn, C. W.; Smith, D. J. *J. Polym. Sci.* **1955**, *17*, 159.
- (21) Brill, R. *J. Prakt. Chem.* **1942**, *161*, 49.
- (22) Brill, R. *Makromol. Chem.* **1956**, *18*, 294.
- (23) Schmidt, G. F.; Stuart, H. A. *Z. Naturforsch.* **1958**, *13A*, 222.
- (24) Atkins, E. D. T. *Macromol. Rep.* **1994**, *A31* (Suppl. 6 & 7), 691.
- (25) Atkins, E. D. T.; Hill, M. J.; Veluraja, K. *Polymer* **1995**, *36*, 35.
- (26) Hirsching, J.; Miura, H.; Gardner, K. H.; English, A. B. *Macromolecules* **1990**, *23*, 2153.
- (27) Wendolowski, J. J.; Gardner, K. H.; Hirsching, J.; Miura, H.; English, A. B. *Science* **1990**, *247*, 431.
- (28) Colletti, M.; Jeno, M.; Mathias, L. J. *Polymer* **1991**, *32*, 332.
- (29) Ramesh, C.; Keller, A.; Eltink, S. J. E. A. *Polymer* **1994**, *35*, 2483.
- (30) Murthy, N. S.; Curran, S. A.; Aharoni, S. M.; Minor, H. *Macromolecules* **1991**, *24*, 3215.
- (31) Radush, H. J.; Stolp, M.; Androsch, R. *Polymer* **1994**, *35*, 3568.
- (32) Colclough, M. L.; Baker, R. *J. Mater. Sci.* **1978**, *13*, 2531.
- (33) Jones, N. A.; Atkins, E. D. T.; Hill, M. J.; Cooper, S. J.; Franco, L. *Macromolecules* **1996**, *29*, 6011.
- (34) Jones, N. A.; Cooper, S. J.; Atkins, E. D. T.; Hill, M. J.; Franco, L. *J. Polym. Sci., Polym. Phys. Ed.* **1997**, *35*, 675.
- (35) Jones, N. A.; Atkins, E. D. T.; Hill, M. J.; Cooper, S. J.; Franco, L. *Polymer* **1997**, *38*, 2689.
- (36) Jones, N. A.; Atkins, E. D. T.; Hill, M. J.; Cooper, S. J.; Franco, L. *Macromolecules* **1997**, *30*, 3569.
- (37) Puiggali, J.; Aceituno, J. E.; Navarro, E.; Campos, J. L.; Subirana, J. A. *Macromolecules* **1996**, *29*, 8170.

MA971895B